

Study of ribbon separation and magnetic reconnection rates

Wenbin Xie^{1,2}, Hongqi Zhang², Jun Lin³, and Haimin Wang⁴

¹Department of Physics, Jilin Normal University,
Postbus 136000, Jilin, China
email: wb_xie@bao.ac.cn

²National Astronomical Observatories Chinese Academy of Sciences,
Postbus 100012 Beijing, China
email: h Zhang@bao.ac.cn

³Yunnan Astronomical Observatory, Chinese Academy of Sciences,
Postbus 650011, Yunnan, China
email: jlin@ynao.ac.cn

⁴New Jersey Institute of Technology,
Postbus NJ07102, Newark
email: haimin@flare.njit.edu

Abstract. We study the correlation between the speed of two-ribbon separation and the magnetic flux density during the 2001 April 10 solar flare. A weak negative correlation is found between the ribbon separation speed (V_r) and the longitudinal magnetic flux density (B_z). In addition, we estimate the magnetic reconnection rate (E_{rec}). Along the flare ribbons, E_{rec} fluctuates in the small range except near the HXR source. The localized enhancement of the reconnection rate corresponds to the position of the HXR source.

Keywords. Solar activity, Solar flares, Solar magnetic fields

1. Introduction

Theoretically speaking, the separation speed of the ribbon expansion is different in the different background magnetic fields (Lin, 2004). Kitahara and Kurokawa (1990) suggested that the two flare ribbons separated much faster in the initial phase of ribbon expansion and then decelerated or even stopped when the $H\alpha$ ribbon front invaded umbrae. Asai *et al.* (2004) found that the separating speed of $H\alpha$ flare kernel decreased when the HXR burst occurred. Miklenic *et al.* (2007) found good temporal correlations between the time profiles of local and global reconnection rate, poynting flux and the HXR flux. Despite of the numerous studies in the past, the following question was not addressed: what is the quantitative relation between the ribbon separation speed and magnetic flux density in flares?

2. Results

On 2001 April 10 an X2.3 two-ribbon flare occurred in the NOAA AR 9415 ($S22^\circ$, $W01^\circ$). The images of the flare ribbon are obtained from the TRACE. We use a magnetogram before the flare eruption obtained with the SOHO / MDI to measure photospheric magnetic flux density. To aid the tracking of the position of the flare ribbons, we choose 46 reference points along the ribbons and mark from L_0 to L_{45} . The locations of reference points L5, L6, L7 and L26, L27, L28, L29 correspond to the left and right HXR sources, respectively.

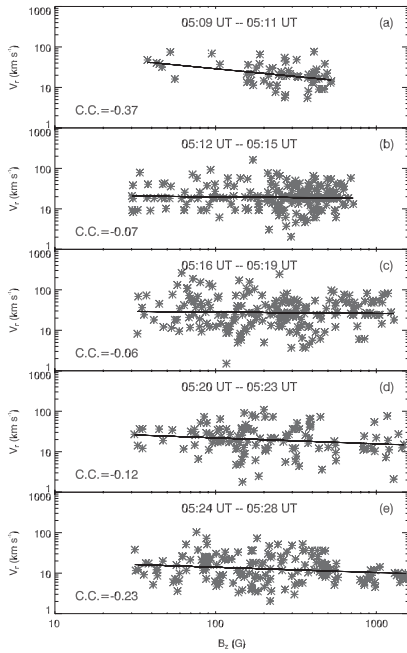


Figure 1. Statistical distribution of V_r s and B_z s in 5 time bins. The solid lines are the fits curves of V_r and B_z : (a), $V_r = 168.5 \times B_z^{-0.38}$; (b), $V_r = 23.8 \times B_z^{-0.04}$; (c), $V_r = 32.4 \times B_z^{-0.03}$; (d), $V_r = 40.8 \times B_z^{-0.15}$; (e), $V_r = 26.4 \times B_z^{-0.13}$.

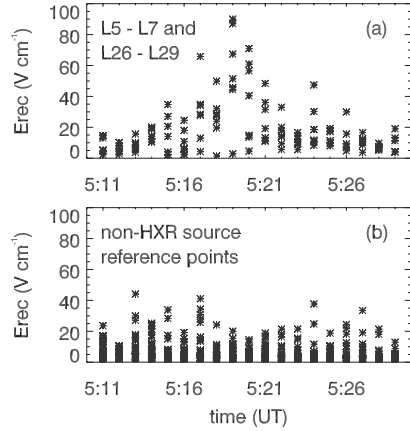


Figure 2. Distribution of E_{rec} at the reference points in the left HXR source (L5-L7) and the right HXR source (L26-L29). (b): Distribution of E_{rec} at the other reference points.

(1) The separating speed of the flare ribbons is negatively correlated with the magnetic field. We analyzed the statistical distribution of the instantaneous speed of ribbon separation and the longitudinal magnetic flux density in each 4-minute time interval after 5:12 UT. Figure 1 shows the scatter plot of V_r s as a function of the absolute value of B_z s in five time bins. The maximum V_r is about 260 km s^{-1} at a location corresponding to B_z s $< 400 \text{ G}$; about 95 km s^{-1} when B_z s are in the range from 400 G to 1300 G , and about 30 km s^{-1} when B_z s $> 1300 \text{ G}$. In Figure 1, the solid line is a fit to the data points in the form of (a) $V_r = 168.5 \times B_z^{-0.38}$, (b) $V_r = 23.8 \times B_z^{-0.04}$, (c) $V_r = 32.4 \times B_z^{-0.03}$, (d) $V_r = 40.8 \times B_z^{-0.15}$, (e) $V_r = 26.4 \times B_z^{-0.13}$.

(2) Along the ribbons, B_z and V_r fluctuate significantly, and the V_r is negatively correlated with the B_z , but E_{rec} fluctuates in the small range except near the HXR source. Figure 2 shows the Distribution of E_{rec} of the reference points in the HXR source (Figure 2a) and the non HXR source (Figure 2b). The localized enhancement of E_{rec} corresponds to the position of HXR source, and the E_{rec} s are weak before and after the peak time of the flare in the position of HXR source.

References

- Asai, A., Yokoyama, T., Shimojo, M., Masuda, S., Kurokawa, H., & Shibata, K. 2004, *ApJ*, 611, 557
- Kitahara, T. & Kurokawa, H. 1990, *SolPhys*, 125, 321
- Lin, J. 2004, *SolPhys*, 222, 115
- Miklenic, C. H., Veronig, A. M., Vršnak, B., & Hanslmeier, A. 2007, *Astron. Astrophys.*, 461, 697